Commensurate Two-Quantum Coherences Induced by Time-Delayed THz Fields

Sharly Fleischer, Robert. W. Field, and Keith A. Nelson

Commensurate Two-Quantum Coherences Induced by Time-Delayed THz Fields

Sharly Fleischer, Robert W. Field and Keith A. Nelson

Department of Chemistry, Massachusetts Institute of Technology, Cambridge, Massachusetts 02139.

Abstract: The interaction of OCS dipolar gas molecules with two time-delayed, single-cycle THz pulses is shown both experimentally and theoretically to induce two-quantum rotational coherences that are significantly enhanced with respect to those induced by one THz pulse, depending on the relative delay of the pulses. The underlying phenomenon is quite general in that it can occur even after a single THz pulse if more than one molecular species is present, since the free induction decay emitted by one species (demonstrated here by atmospheric water vapor) can provide the second field interaction for the other.

It has long been known that molecular rotational coherences can be driven by a single-cycle terahertz (THz) electromagnetic field that interacts resonantly with a molecular dipole moment [1,2,3,4] or by a femtosecond optical field that interacts nonresonantly with a molecular polarizability anisotropy [5,6]. For linear molecules, a single THz field interaction with the molecular dipoles couples initial and final rotational levels, J and $J' = J \pm 1$. Under ambient conditions with many occupied levels, the superposition of such 1-quantum coherences (1QCs) whose frequencies $\omega(\rho_{J,J+1}) = 2(J+1)Bc$ are multiples of $2Bc$, leads to equally spaced "revivals" of short-lived net molecular orientation, $<\cos\theta>(t)$, with revival period $T_{\text{rev}} = 1/2Bc$ (B is the molecular rotational constant in cm^{-1} units, c is the speed of light in vacuum, and θ is the angle between the dipole moment and the THz field polarization). The revivals are revealed through THz free induction decay (FID), which is expressed as corresponding bursts of coherent THz emission from the instantaneously oriented sample [1,2,3]. Two interactions with an ultrashort optical field (which exerts torque through impulsive stimulated rotational Raman scattering) couple initial and final levels with $J'' = J \pm 2$, and the superposition of 2-quantum coherences (2QCs) whose frequencies are given by $\omega(\rho_{J,J+2}) = (4J+6)Bc$, result in short-lived modulations of molecular alignment, $<\cos^2\theta>(t)$, separated by $T_{\text{rev}}/2$, which have phases reversed between successive occurrences. With intense optical pulses, many successive light-matter interactions can couple large numbers of levels J, $J \pm 2$, $J \pm 4$, etc., yielding in some cases a high degree of alignment during the recurrences and also transferring population among rotational levels of the same parity. The alignment recurrences and the non-thermal rotational distributions[7,8] are revealed through time-dependent optical birefringence, measured with variably delayed probe pulses. Several key applications such as high harmonic generation (HHG)

[9,10,11,12] and molecular frame photoelectron angular distribution (MFPAD) [13,14,15] spectroscopies make use of optically induced anisotropic angular distributions (alignment and orientation prepared by a single pulse, a sequence of pulses [16,17], DC fields [18] or mixed field excitations[19,20,21,22]), while others aim at coherently controlled molecular rotation for purposes of quantum information [23], chemical selectivity [24,25], preferred direction of rotation [26,27,28,29,30,31] etc., induced by femtosecond pulse sequences with varying relative delays and polarizations as well as shaped optical pulses [31,32,33].

In the initial weak-field THz experiments [2,3], the only detectable signals were those resulting from a single light-matter interaction, i.e. from 1QCs with $J' = J \pm 1$ (described by the $\Delta J = \pm 1$ off-diagonal density matrix elements, $\rho_{J,J'}(t)$). Recently [34], OCS molecules were driven by single-cycle THz pulses of sufficient strength to generate not only 1QCs (detected as THz FIDs) but also 2QCs and non-thermal rotational state distributions (detected as optical birefringence) that result from two successive light-matter interactions. Outside of the weak-field limit, it is of interest to explore THz excitation strategies that could enhance control over orientation and/or alignment [35], including a combination of THz and optical fields [36,37,38]. More generally we wish to explore strategies for coherent control over multilevel systems, exemplified here by control over rotational coherences and populations. Apart from the strong-THz field goals such as high degrees of molecular orientation or alignment for applications like HHG or MFPAD our objectives include two-dimensional rotational spectroscopy for revealing the couplings between different rotational degrees of freedom of (non-linear) molecules, and transient rotational spectroscopy of molecular species formed as reaction intermediates or products in highly non-thermal rotational distributions.

We present experimental results from polar OCS molecules driven by time-delayed THz pulse pairs. *We show that two THz-molecule interactions at widely separated times can induce far larger transient birefringence responses, indicating far larger 2QCs, than two interactions within a single short THz pulse, and that there is an optimal time delay for the largest response.* We further show that in the presence of atmospheric water vapor, a closely related effect arises from one single-cycle THz excitation pulse followed by the THz FID from water that it induces, which in turn acts on the OCS molecules. Thus the underlying phenomenon may occur whenever a strong THz pulse irradiates multiple molecular species, even when (as in the present case with water vapor outside the OCS cell) the different species are separated spatially.

The experimental setup is shown in the Online Supplementary Material (OSM)-1. Two single-cycle THz pulses are generated in a nonlinear crystal by two variably delayed optical pulses, and the time-dependent birefringence of the medium is probed by a weak optical pulse [39]. Figure 1 shows the time-dependent birefringence induced in an OCS gas sample by two THz pulses delayed by $\Delta \tau = 29 \, ps$. The blue and green arrows label the signal components that can be attributed to the first or second THz excitation pulse, respectively. Thus the blue arrows indicate a rise of the background signal at $t = 0$, when the first THz pulse arrives at the sample, and

birefringence modulations at $T_{rev}/2$ and T_{rev}. (For OCS, $B = 0.203$ cm^{-1} and $T_{rev} = 82.2$ ps). The slowly varying background signal is due to the non-thermal rotational state distribution, while the modulations due to rotational 2QCs are characteristically short-lived [34]. The green arrows indicate similar responses to the second THz pulse, all of which are delayed 29 ps relative to their counterparts, which were induced by the first pulse. The much stronger signal modulations (~35x relative to those induced by either of the pulses alone) at 56, 97, 138, and 179ps appear only when both THz pulses are present, and are the focus of the present work. For a simulated result, see OSM-2.
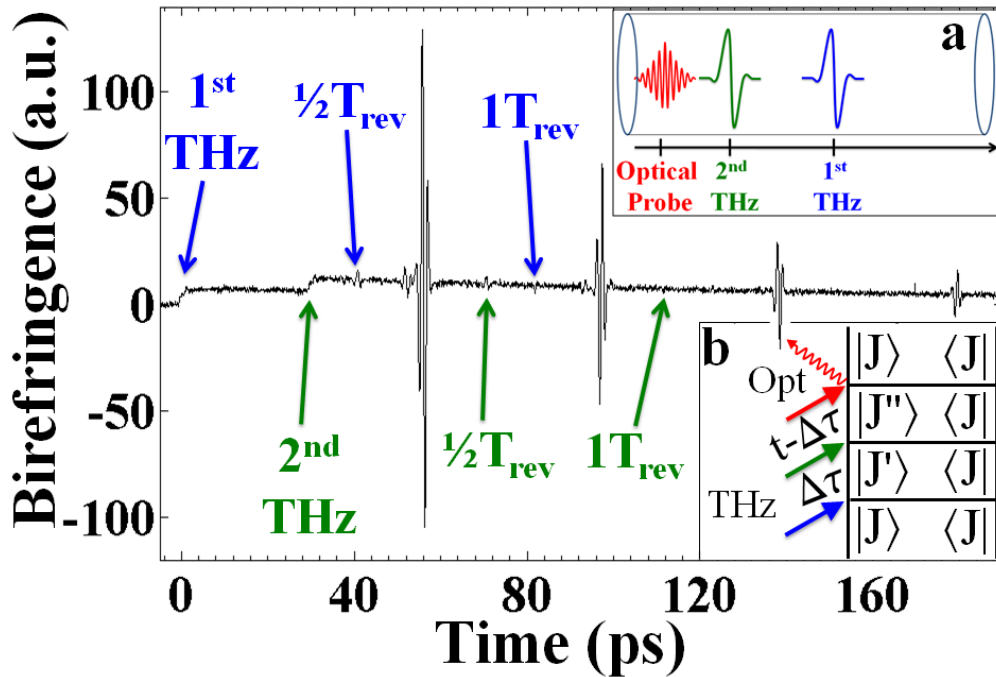

Figure 1: Experimentally measured birefringence induced in a 500-torr OCS gas sample at room temperature, produced by interactions with two single-cycle THz fields. Inset (a) is a schematic representation of the fields used. The multiple-cycle optical probe pulse duration (~ 100 fs, red) is actually shorter than the THz pulse durations (~ 1.5 ps, green and blue). Inset (b) is a Feynman diagram showing the two THz excitation fields (blue and green) that produce 1QCs and 2QCs in succession, and the optical fields (red) used to probe the 2QCs.

We refer to the strong modulations as "Commensurate Two-THz Revivals" (CTTR) for reasons that will become clear shortly. Simulated birefringence responses of the OCS gas at 300 K during and after its interaction with two single-cycle, equal-amplitude THz pulses with field profiles $E(t)$ are calculated based on the dipolar interaction potential, $V(\theta, t) = -\mu E(t) \cos(\theta)$, where μ is the molecular dipole moment. From the calculations, conducted for various THz field amplitudes, we found the CTTR signal level to be linearly proportional to each field amplitude,

$A_{CTTR} \propto E_1 \cdot E_2$, indicating one field↔molecule interaction with each pulse, as further described in OSM-3.

Figure 2a shows seven time-dependent birefringence sweeps like the one shown in Fig. 1, from 180 torr OCS, with the first THz excitation pulse arriving at $t = 0$ in all cases and the second THz pulse arriving after a delay of 10, 20,..., 70 ps. The plot of all seven sweeps together illustrates the dependence of the CTTR signals on the time interval between THz excitation pulses. Consistent with Fig. 1, the CTTR signals induced by each pulse-pair with separation $\Delta\tau$ appear at times $(T_{rev} + \Delta\tau)/2$, i.e. following the second pulse by $(T_{rev} - \Delta\tau)/2$. Thus successive sweeps with pulse-pair separations, $\Delta\tau$, incremented in steps of 10 ps show CTTR signals that are incremented by 5 ps. Figure 2 also shows that the CTTR signals are largest in the fourth sweep, with a delay of $\Delta\tau = 40$ ps.
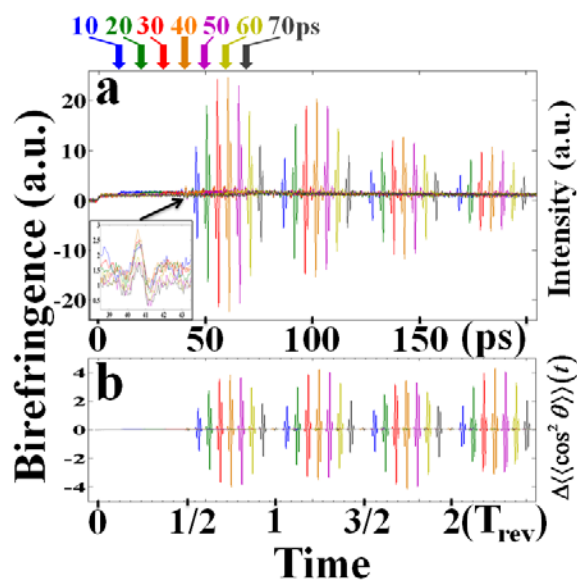
Figure 2: a) Seven experimental data sets illustrate THz-induced time-dependent birefringence in 180 torr OCS at 300 K for seven different delays (color-coded) between two single-cycle THz excitation pulses. The arrows mark the arrival time of the second pulse. The inset shows the birefringence modulation at $\frac{1}{2}T_{rev}$ (41ps for OCS molecules) induced by the first THz pulse in each data set. b) Simulation results for the time-dependent change in alignment factor (in arbitrary units) for the experimental sample parameters. The simulation includes the centrifugal distortion of OCS but does not take dephasing or relaxation processes into account.

Figure 2b depicts the results of seven calculations like those shown in OSM-2, conducted with the time intervals $\Delta\tau = 10, 20, ..., 70$ ps used to generate the experimental results that are displayed in figure 2a. The trends in CTTR signal timing and amplitude as a function of the time interval are clearly in good agreement. The CTTR signal phase at longer times (150-200 ps) is slightly shifted with respect to the phase at shorter times (in both experimental and simulated data) due to the centrifugal distortion of OCS ($D = 4.33 \cdot 10^{-8} cm^{-1}$), leading to slightly incommensurate rotational periods of the different states [40,41,42]. Although the calculations

were not performed perturbatively, the results can be understood in terms of successive independent interactions between THz fields and molecular dipoles.

The first THz field interaction with the molecular dipoles induces 1QCs between all of the adjacent rotational states with transition frequencies within the pulse bandwidth. The field-free evolution of these coherences is described by the $\Delta J = \pm 1$ off-diagonal density matrix elements

$$\rho_{JJ'}(t) = c_J^* c_{J'} \exp(-i\omega_{JJ'}t) \text{ , where } \omega_{JJ'} = (E_{J'} - E_J)/\hbar = 2\pi Bc(2J+2) = 2\pi(J+1)/T_{rev} \qquad (1)$$

the superposition of which for multiple initial J levels manifests net orientation modulations under field-free conditions. It was shown that with sufficient field strengths, this rotational motion is accompanied by measurable degrees of alignment [34]. Classically, the small extent of net alignment after the interaction with one THz pulse can be understood in terms of the interaction potential, $V_{THz} \propto \cos\theta$, and the resulting torque, $\tau_{THz} \propto -\sin\theta$, which rotates molecules with dipoles already pointing partly in the $+z$ direction ($-\pi/2 \le \theta_0 \le \pi/2$) further toward that direction, and rotates molecules with dipoles pointing partly in the $-z$ direction toward the xy plane, i.e. away from the z axis. *The two groups of responses both contribute to net orientation in the $+z$ direction but make cancelling contributions to alignment along the z axis.* A related argument regarding the small degrees of alignment induced through the dipole interaction was made in theoretical work by Henriksen [35].

The second THz pulse arrives after time delay $\Delta\tau$ and interacts with the previously excited molecules, initiating additional 1QCs, which yield

$$\rho_{JJ'}(t > \Delta\tau) = c_J^* c_{J'} [1 + \exp(-i\omega_{JJ'}\Delta\tau)] \exp[-i\omega_{JJ'}(t - \Delta\tau)] \qquad (2)$$

Figure 3c shows simulated 1QC amplitudes after two field interactions with different delays. If the two interactions are time-coincident or delayed by an integer number of revival times ($\Delta\tau = nT_{rev}$ with $n = 0,1,2,...$), then all of the 1QCs initiated by the first interaction are in phase when the second interaction occurs and the 1QC amplitudes generated by the two interactions superpose constructively for all J (figure 3c left-hand column). If the two interactions are delayed by $T_{rev}/2$ (or by $\Delta\tau = (n+1/2)T_{rev}$), then the 1QCs with even and odd initial J values are out of phase when the second interaction occurs, resulting in constructive superposition for odd J and destructive superposition for even J (figure 3c right-hand column). Intermediate delay times (middle column) yield patterns of constructive and destructive superposition that are more complex yet entirely predictable based on the 1QC phases at the time of the second interaction.

The second field interaction also induces 2QCs with magnitudes and phases depending on its time delay, $\Delta\tau$. These are represented by the $\Delta J = \pm 2$ off-diagonal density matrix elements:

$$\rho_{JJ''}(t > \Delta\tau) = c_J^* c_{J''} \exp\left[-i\omega_{JJ''}(t - \Delta\tau) - i\omega_{JJ'}\Delta\tau\right] \text{ with } \omega_{JJ''} = 2\pi Bc(4J+6) = 2\pi(2J+3)/T_{rev}$$
(3)

The magnitudes of these terms will be discussed later, but let us first consider the phase accumulated by each 2QC at the time of the birefringence measurement, t. There are two contributions: the phase accumulated by the 1QC until time $\Delta\tau$, and the phase accumulated by the 2QC from time $\Delta\tau$ until time t. The CTTR signals appear when the 2QCs in Eq.3 are all in phase, i.e when the accumulated phases,

$$\xi_{(J,J+2)} = \omega_{JJ''}(t - \Delta\tau) + \omega_{JJ'}\Delta\tau = \left[2\pi J(2t - \Delta\tau) + 3\pi(2t - \Delta\tau) - \pi\Delta\tau\right]/T_{rev}$$
(4)

are independent of the J quantum number except for increments of 2π. This occurs when $2t - \Delta\tau = nT_{rev}$, yielding for the first two CTTR appearance times

$$t_1 = \frac{T_{rev} + \Delta\tau}{2}, \quad \xi_{(J,J+2)}(t_1) = 2\pi J + 3\pi - \pi\Delta\tau/T_{rev}$$
(5)

$$t_2 = \frac{2T_{rev} + \Delta\tau}{2}, \quad \xi_{(J,J+2)}(t_2) = 4\pi J + 6\pi - \pi\Delta\tau/T_{rev}$$
(6)

The π phase shift is observed between successive birefringence modulations in the experimental and simulated data in figures 1,2 and has been previously observed in birefringence modulation induced by either optical [43] or THz [34] fields. The 2QC phases accumulate at twice the rate of the 1QC phases, which is why the time interval between successive 2QC signal appearances is $T_{rev}/2$ while that between the 1QC appearances is T_{rev}. The first 2QC signal follows the second field interaction by $(T_{rev} - \Delta\tau)/2$ rather than by $T_{rev}/2$ because of the phase already accumulated by the 1QC during the time interval $\Delta\tau$. Note that the CTTR is not an "echo" or rephasing signal: the sign of the phase accumulation does not change after the second field interaction.

The amplitude of the CTTR signal observed for a given delay $\Delta\tau$ between the two fields depends on the amplitudes of the 2QC terms in Eq. (3), each of which results from interference between two different quantum mechanical pathways. The second field generates the 2QC $\rho_{JJ''}$ from either of the two 1QCs $\rho_{JJ'}$ or $\rho_{J'J''}$ that are generated by the first field. For $\Delta\tau = n \cdot T_{rev}$ the destructive contributions of these two terms to $\rho_{JJ''}$ corresponds to the classical picture of alignment cancellation introduced previously ($\Delta\tau = 0$) and is indicated by the small birefringence signals observed experimentally and in the simulation results shown in figure 3d (left-hand column). However, due to their different frequencies, $\omega_{JJ'} = 2\pi(J+1)/T_{rev}$ and $\omega_{J'J''} = 2\pi(J+2)/T_{rev}$, at $\Delta\tau = T_{rev}/2$ the two 1QC terms are exactly π phase-shifted and they contribute constructively to the 2QC term, $\rho_{JJ''}$, as manifest in both

the simulation results (figure 3d, right-hand column) and in the largest observed CTTR signals. At intermediate times, the CTTR signal is reduced due to partial destructive contributions of $\rho_{JJ'}$ and $\rho_{J'J''}$ (figure 3d, middle column).
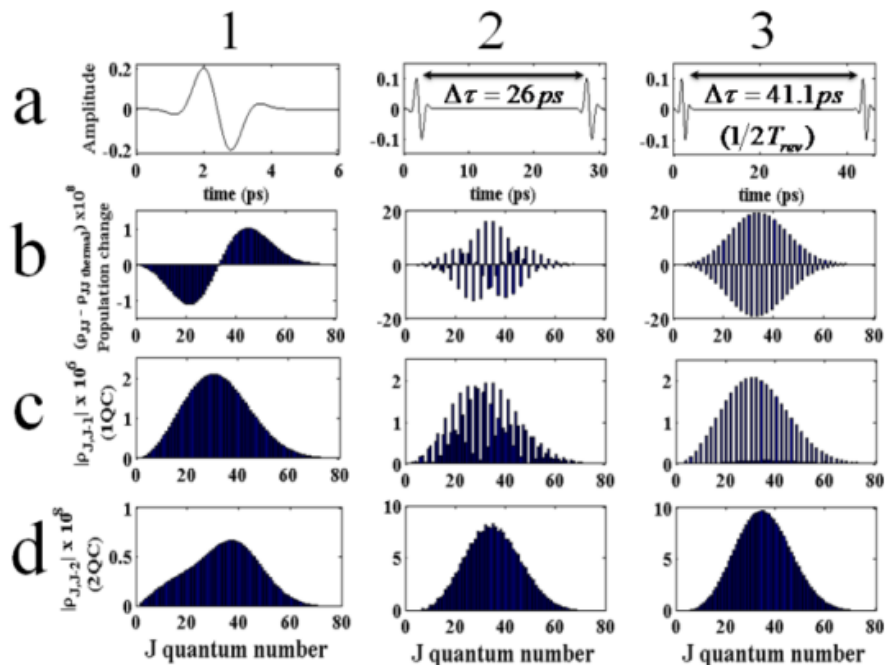

Figure 3: Numerical calculations of: (b) change in populations, (c) 1QC magnitudes, and (d) 2QC magnitudes following the interaction with (1a) a single THz field (with twice as strong amplitude relative to the following fields), (2a) two THz fields with delay of 26 ps, and (3a) two THz fields delayed by $1/2T_{rev}$ (41.1 ps), all calculated for OCS at 300K, and presented for the case of 'm'=0. (see movies in OSM-4).

Figure 3b shows the change in population for each of the J states that is induced by the two fields. The J-dependent patterns of population change are very different for different delays. For $\Delta\tau=0$, the population is shifted uniformly from low J to high J states. For $\Delta\tau=T_{rev}/2$, the population is transferred selectively from odd J to even J states (see OSM-5). At intermediate delay times, a more complicated but systematic J-dependent pattern is observed.

A closely related phenomenon is observed when one single-cycle THz field is applied to an OCS gas sample, but unlike the earlier measurements, the ambient atmosphere outside the OCS cell is not purged of water vapor. The OCS sample is irradiated by the single-cycle pulse, followed by the continuous FID from water, which provides the second THz field interaction. The results, shown and discussed further in section OSM-6, reveal strong CTTR signals that oscillate at twice the water FID frequency. Thus 2-quantum coherences may be induced whenever a single strong THz field irradiates multiple polar molecular species, with the FID from any species providing the second field interaction for any other species that are downstream in the beam path.

We note that in the present demonstration of control over multiple 2QCs, using THz fields of moderate strength (~ 50 kV/cm) and molecules at room temperature, the maximum induced change in alignment $\Delta < \cos^2\theta >$ was $\sim 10^{-3}$– significantly smaller than values often induced by optical pulses. Far higher tabletop THz field strengths (> 1 MV/cm [44]) can be used on samples at lower temperatures in order to drive substantially greater degrees of alignment.

In summary, we have shown that two properly delayed THz pulses induce significantly enhanced transient birefringence relative to that induced by a single THz pulse. By varying the delay between pulses, one can control the magnitudes and relative phases of the 2QCs in a multilevel rotational system. Selective population transfer between even and odd rotational states, which is forbidden via optical excitation, becomes possible through the interaction of molecular dipoles and THz fields. The experimental results agree closely with numerical calculations. The present results provide an instructive example of THz coherent control over rotational state populations and coherences. Of special interest using the presented excitation scheme are molecules showing more than one fundamental rotational axis, in which CTTR signals may reveal the coupling between different rotational degrees of freedom.

[1] D. Bigourd, G. Mouret, A. Cuisset, F. Hindle, E. Fertein, and R. Bocquet, *Opt. Comm.* **281**, 3111–3119 (2008)
[2] H. Harde, S. Keiding, D. Grischkowsky, *Phys. Rev. Lett.* **66**, 1834-1837 (1991).
[3] H. Harde and D. Grischkowsky, *J. Opt. Soc. Am. B* **8**, 8 (1991).
[4] M. Machholm and N. E. Henriksen, *Phys. Rev. Lett.* **87**, 193001 (2001).
[5] H. Stapelfeldt, and T. Seideman, *Rev. Mod. Phys.* **75**, 543 (2003)
[6] I. Sh. Averbukh and R. Arvieu, *Phys. Rev. Lett.* **87**, 163601 (2001).
[7] James P. Cryan, Philip H. Bucksbaum, and Ryan N. Coffee, *Phys. Rev. A* **80**, 063412 (2009)
[8] S. Ramakrishna, and T. Seideman, *PRL* **95**, 113001 (2005)
[9] R. Velotta, N. Hay, M.B. Mason, M. Castillejo, and J.P. Marangos, *Phys. Rev. Lett.* **87**, 183901 (2001).
[10] J. Itatani, J. Levesque, D. Zeidler, H. Niikura, H. Pepin, J. C. Kieffer, P. B. Corkum, and D. M. Villeneuve, *Nature* **432**, 867 (2004).
[11] H. Soifer, P. Botheron, D. Shafir, A. Diner, O. Raz, B. D. Bruner, Y. Mairesse, B. Pons, and N. Dudovich, *PRL* **105**, 143904 (2010).
[12] B. K. McFarland, J. P. Farrell, P. H. Bucksbaum, and M. Gühr, *Science* **322**, 1232 (2008).
[13] Albert Stolow, Annu. Rev. Phys. Chem **54** 89-119 (2003).
[14] M. Meckel, D. Comtois, D. Zeidler, A. Staudte, D. Pavičić, H. C. Bandulet, H. Pépin, J. C. Kieffer, R. Dörner, D. M. Villeneuve, P. B. Corkum, *Science* **320**, 1478 (2008).
[15] L. Holmegaard, J. L. Hansen, L. Kalhøj, S. L. Kragh, H. Stapelfeldt, F. Filsinger, J. Küpper, G. Meijer, D. Dimitrovski, M. Abu-samha, C. P. J. Martiny, and L. B. Madsen, *Nature Phys.* **6**, 428-432 (2010).
[16] M. Leibscher, I. Sh. Averbukh, and H. Rabitz, *Phys. Rev. Lett.* **90**, 213001 (2003)

[17] C. Z. Bisgaard, M. D. Poulsen, E. Peronne, S. S. Viftrup, and H. Stapelfeldt, *Phys. Rev. Lett.* **92**, 173004 (2004).

[18] B. Friedrich and D. Herschbach, *Nature* **353**, 412-414 (1991).

[19] L. Holmegaard, J. H. Nielsen, I. Nevo, H. Stapelfeldt, F. Filsinger, J. Küpper, and G. Meijer *Phys. Rev. Lett.* **102**, 023001 (2009).

[20] A. Goban, S. Minemoto, and H. Sakai, *Phys. Rev. Lett.,* **101**, 013001 (2008).

[21] O. Ghafur, A. Rouzée, A. Gijsbertsen, W. K. Siu, S. Stolte and M. J. J. Vrakking, *Nature Phys.* **5**, 289-293 (2009).

[22] S. De, I. Znakovskaya, D. Ray, F. Anis, Nora G. Johnson, I. A. Bocharova, M. Magrakvelidze, B. D. Esry, C. L. Cocke, I. V. Litvinyuk, and M. F. Kling, *Phys. Rev. Lett* **103**, 153002 (2009).

[23] K. F. Lee, D. M. Villeneuve, P. B. Corkum and E.A. Shapiro, *Phys. Rev. Lett*, 93, 233601 (2004).

[24] S. Fleischer, I.Sh. Averbukh, and Y. Prior, *Phys.Rev. A* **74**, 041403 (2006).

[25] S. Fleischer, I. Sh. Averbukh, and Y. Prior, *Phys. Rev. Lett.* **99**, 093002 (2007).

[26] Joanna Karczmarek, James Wright, Paul Corkum, and Misha Ivanov, *Phys. Rev. Lett.* **82**, 3420–3423 (1999)

[27] L. Yuan, S. W. Teitelbaum, A. Robinson, and A. S. Mullin, *PNAS* **108**, 6872-6877 (2011)

[28] Sharly Fleischer, Yuri Khodorkovsky, I. Sh. Averbukh and Yehiam Prior. *New Journal of Physics* **11,** 105039 (2009).

[29] Yuri Khodorkovsky, Kenta Kitano, Hirokazu Hasegawa, Yasuhiro Ohshima, and Ilya Sh. Averbukh, *Phys. Rev. A* **83**, 023423 (2011).

[30] K. Kitano, H. Hasegawa, and Y. Ohshima, *Phys. Rev. Lett.* **103**, 223002 (2009).

[31] S. Zhdanovich , A. A. Milner, C. Bloomquist,J. Floss, I. Sh. Averbukh, J. W. Hepburn, and V. Milner, *Phys. Rev. Lett.* **107**, 243004 (2011).

[32] E. Hertz, A. Rouzee, S. Guerin, B. Lavorel, and O. Faucher, *Phys. Rev. A* **75**, 031403 (2007).

[33] M. Renard, E. Hertz, S. Guerin, H. R. Jauslin, B. Lavorel, and O. Faucher, *Phys. Rev. A* **72**, 025401 (2005).

[34] Sharly Fleischer, Yan Zhou, Robert W. Field, and Keith A. Nelson, *Phys. Rev. Lett.* **107**, 163603 (2011)

[35] Niels E. Henriksen, Chem. Phys. Lett. **312**, 196-202 (1999)

[36] Erez Gershnabel, Ilya Sh. Averbukh, and Robert J. Gordon, Phys. Rev. A, **73** 061401 (2006).

[37] Erez Gershnabel, Ilya Sh. Averbukh, and Robert J. Gordon, Phys. Rev. A, **74** 053414 (2006).

[38] Kenta Kitano, Nobuhisa Ishii, and Jiro Itatani, Phys. Rev. A **84**, 053408 (2011)

[39] B. Lavorel, O. Faucher, M. Morgen, and R. Chaux, *J. Raman Spectrosc.* **31**, 77 (2000).

[40] N. Owschimikow, F. Königsmann, J. Maurer, P. Giese, A. Ott, B. Schmidt, and N. Schwentner, *J. Chem. Phys.*, **133**, 044311 (2010).

[41] M. Morgen, W. Price, L. Hunziker, P. Ludowise, M. Blackwell, and Y. Chen, *Chem. Phys. Lett.* **209**, 1-9 (1993).

[42] D. W. Broege, R. N. Coffee, and P. H. Bucksbaum, *Phys. Rev.A*, **78**, 035401 (2008)

[43] S. Fleischer, I. Sh. Averbukh , and Y. Prior, *J. Phys. B* **41**, 074018 (2008).

[44] H. Hirori, F. Blanchard, and K. Tanaka, *Appl. Phys. Lett.* **98**, 091106 (2011).